Journal of Electrostatics, 20 (1987) 95-108
Elsevier Science Publishers B.V., Amsterdam — Printed in The Netherlands

ARC PROPAGATION, EMISSION AND DAMAGE ON SPACECRAFT DIELECTRICS: A REVIEW

K.G. BALMAIN

Department of Electrical Engineering, University of Toronto, Toronto, Ontario M5S 1A4 (Canada)

(Received September 25, 1986; accepted in revised form June 1, 1987)

Summary

This paper is a review of the literature on the subject of arc discharges on spacecraft dielectric materials that have become charged by energetic electrons and ions. The results discussed will be mainly from laboratory measurements of the properties of these arc discharges. Arcs resulting from the charging of spacecraft dielectrics can be extremely strong because the charge over a large area is mobilized through the phenomenon of arc propagation. The resultant damage patterns on the dielectric will be shown to be related to the arc patterns, and to the optical anisotropy and crystallinity of the material. The evidence for dielectric melting is suggestive of likely contamination of nearby surfaces. The effectiveness of arc barriers sheds light on arc propagation mechanisms. Coupling to external circuits can be deduced from blowoff calculations and from near-field measurements of arc currents. Exposed dielectric edges contributed to charge accumulation and arc triggering. Broad-spectrum, high-energy incident electrons can cause charging and discharging internal to the spacecraft.

1. Introduction

Charge accumulation in spacecraft dielectric materials is believed to be responsible for arc breakdown, strong electromagnetic interference, and consequent "operational anomalies" or sometimes irreversible component failures on operational synchronous-orbit satellites. The possibility that the magnetospheric hot-plasma environment could cause such failures has led to two books [1,2], five conference proceedings [3–7] and many journal publications. The quiet and disturbed magnetosphere has been reviewed and its properties correlated convincingly with anomaly occurrences [8–16]. Even in Jupiter's magnetosphere, discharges probably caused the unexpected "power-on resets" observed on the Voyager spacecraft, forcing the design of corrective measures for the planned Galileo flight past Jupiter [17]; these additional corrective measures were intended to reduce internal charging due to penetrating high-energy electrons, because external charging had already been eliminated through the choice of exposed materials.

0304-3886/87/$03.50

Few satellites have been instrumented to observe charging/discharging phenomena. Although not intended for this purpose, particle spectrometers measured whole-satellite charging as early as 1972 [18]. Much later, a satellite to study Spacecraft Charging at High Altitude (SCATHA, or P78-2) was launched, carrying a selection of exposed materials [19] and appropriate instruments. The resulting measurements have been reviewed [20–23] showing that arc discharges actually did occur. However, relative to laboratory measurements, these discharges in space were weaker than expected and they occurred at unexpectedly low values of surface potential, a result which provoked a re-examination of laboratory simulation techniques to be discussed further in Section 3.

Laboratory measurements of arc phenomena are, of course, much easier to make than space measurements. Motivated by concern over satellite failures, researchers started in about 1972 to expose back-metallized sheets of thermal-blanket polymer to monoenergetic electron beams up to about 25 keV. They observed arc discharges and saw tree-shaped damage patterns which they soon realized were miniatures of the large Lichtenberg figure damage patterns observed much earlier by Gross [24,25].

2. Classification of arcs and damage tracks

The arcs observed on polymer sheets were multi-forked and lightning-like (Fig. 1), often extending over most of the exposed surface area and appearing to start at an exposed edge or at a point of bulk breakdown to the metallized backing (a "punchthrough") [26]. Arcs that begin at a punchthrough are generally more frequent and weaker than those that begin at an edge, probably because less accumulated charge is needed to produce breakdown fields and trigger an arc in the vicinity of a punchthrough. Whatever the starting point, arc patterns often appear to have a preferred direction (Fig. 2), which has been correlated with the direction of microscopic damage tracks (Fig. 3), with the slow axis of optical anisotropy, and with the microscopic "brick and mortar" patterns revealed by surface etching [27]; these direction surface properties are due to the mechanical stretching which is part of the process of manufacturig some types of thin polymer sheets. It has also been noted [28] that, if an exposed polymer sheet edge is parallel to the principal optical axis, the breakdown threshold of beam energy is the same as if the edge were not exposed, while for other orientations the threshold is lower. In Refs. [29] and [30] there are papers [29a,30a,30b] that show many types of material damage, especially sub-surface tunnels, surface grooves, and tunnel eruptions with clear evidence of localized melting (Fig. 4). Mass-spectroscopic analysis [31] provides evidence that surface breakdown on polymers results in emission of light hydrocarbons and fluorocarbons. Quartz optical solar reflectors arc only at their edges where edge chipping is observed [32]; this is not surprising because

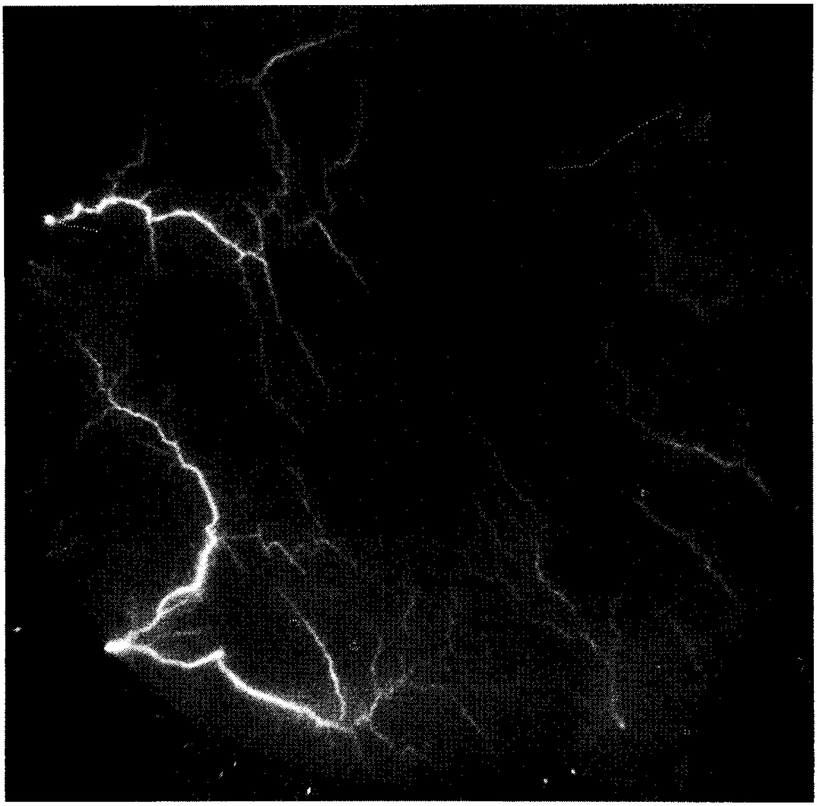

Fig. 1. Arc discharge on Mylar sheet specimen over a grounded substrate and covered by a grounded mask with a circular aperture [41].

calculations predict high charge and field concentrations near dielectric edges exposed to an electron beam [33]. Discharges have also been detected under a conducting coating of indium tin oxide on quartz [34]. As well, there is a possibility that electrical pre-charge could be triggered into an arc discharge state by external fields such as X-rays [35,36]. Recently arc discharge damage has been reviewed [37] and the similarity between polymer arcs and atmospheric lighting has been explored in depth [38].

3. Arc discharge dependence on material dimensions and incident beam properties

For a thin sheet of polymer over a conducting substrate, laboratory experiments showed that the peak substrate replacement current is approximately proportional to the square root of the exposed area, over a range from 1000 A at 1 m^2 to 1/10 A at 10^{-8} m^2, the latter microscopic area having been defined

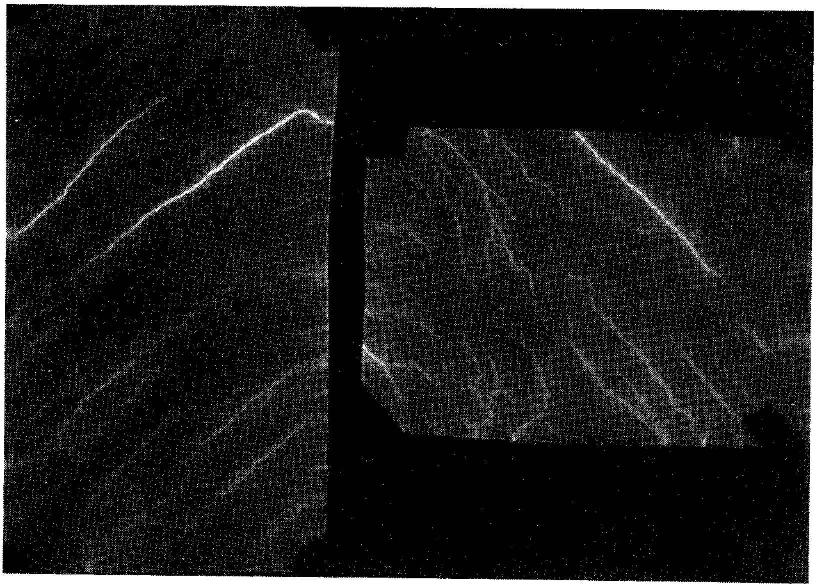

Fig. 2. Simultaneous arcs on two Mylar specimens which were cut from the same sheet, and one of which was rotated 90° [30b].

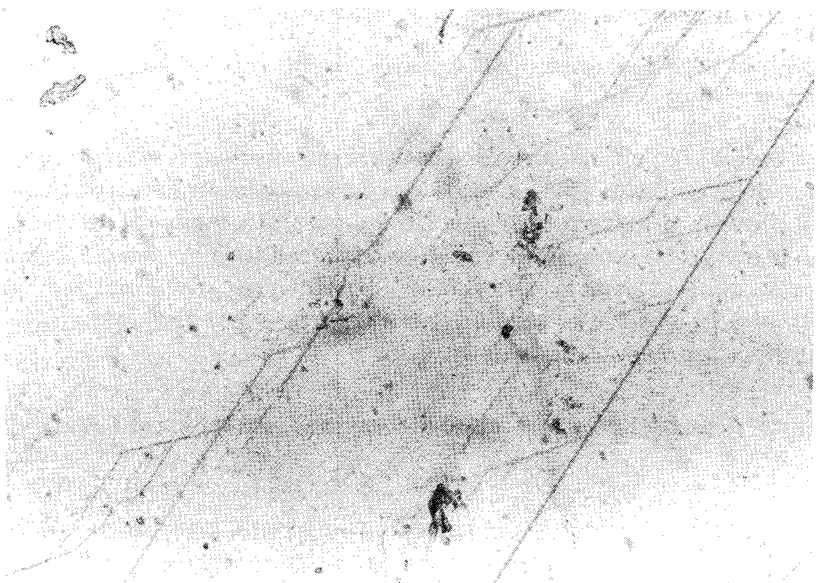

Fig. 3. Straight damage tracks on Mylar sheet. Photograph width is 450 μm [27].

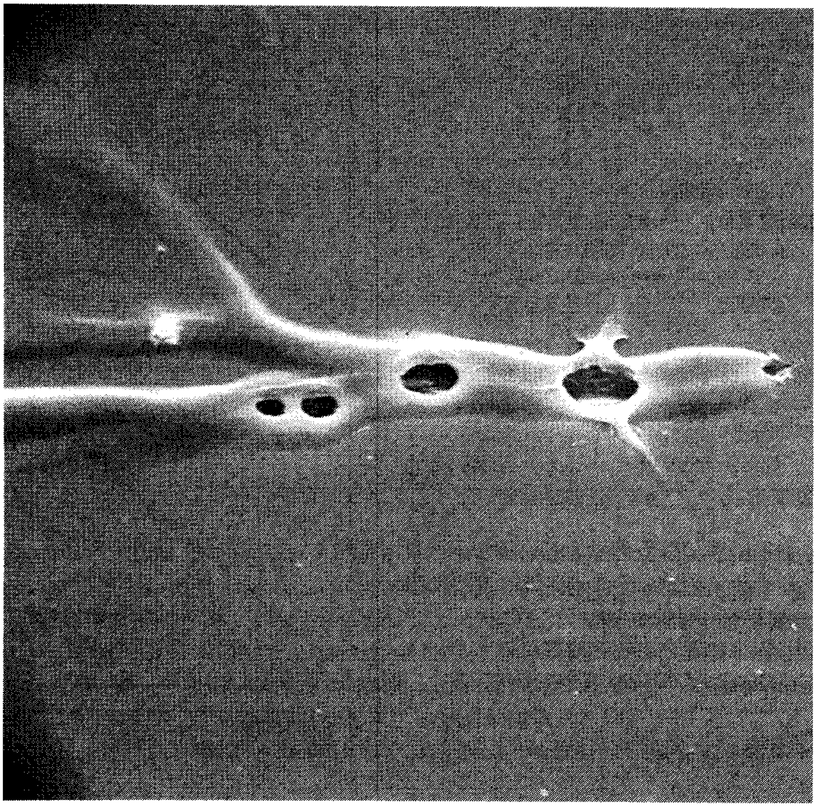

Fig. 4. Near-surface damage tunnel with apparently melted eruption holes [29a].

by partially focussing the incident electron beam [39]. Further refinement of the area-scaling experiments [40–42] confirmed this square-root-area dependence (Fig. 5), and, moreover, showed that the charge released (the time integral of the substrate current) is proportional to the exposed area (Fig. 6) and the arc duration is proportional to the square root of the area (Fig. 7). The charge proportionality to area is what one would expect, assuming that all the charge (or at least a constant fraction of it) is cleaned off during each discharge. The duration proportionality to linear dimension (square root area) implies a well-defined arc propagation velocity across the surface. Finally, the peak current proportionality to linear dimension is consistent with the concept of discharge by an advancing wavefront, so that the instantaneous current is proportional to the wavefront width, which has a maximum value of the order of the specimen's linear dimensions. Other experiments on discharge scaling have involved the measurement of radiated signal spectra [43,44], with the conclusions that the radiated energy is proportional to the peak substrate current, the radiated energy is inversely proportional to the duration of the sub-

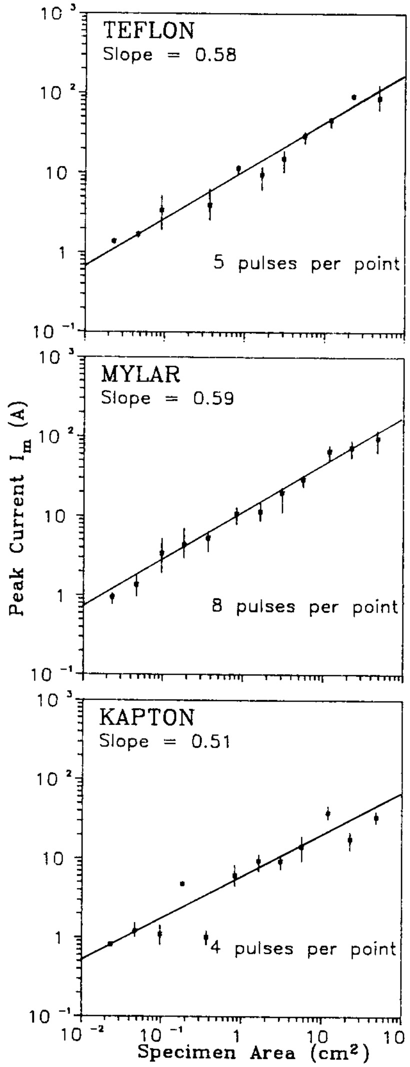

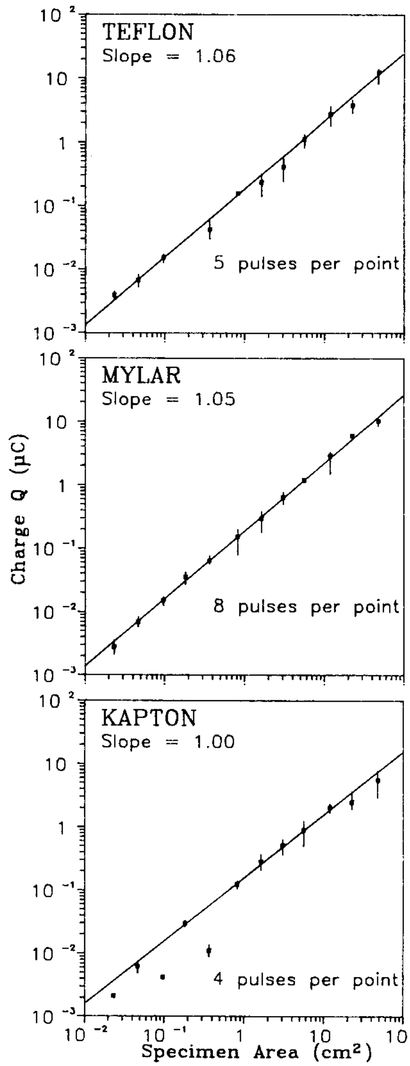

Fig. 5. The peak substrate current during an arc discharge, showing its approximately square-root dependence on specimen area [42].

Fig. 6. The total charge released to ground from the substrate during an arc discharge, showing its approximate proportionality to specimen area [42].

strate current pulse, and the radiated spectrum is a function of area. A dependence of peak current on incident electron flux has been observed on Kapton [45,46] and traced to material conductivity effects which are significant at low fluxes [33]. Specimen thickness was found to influence charging

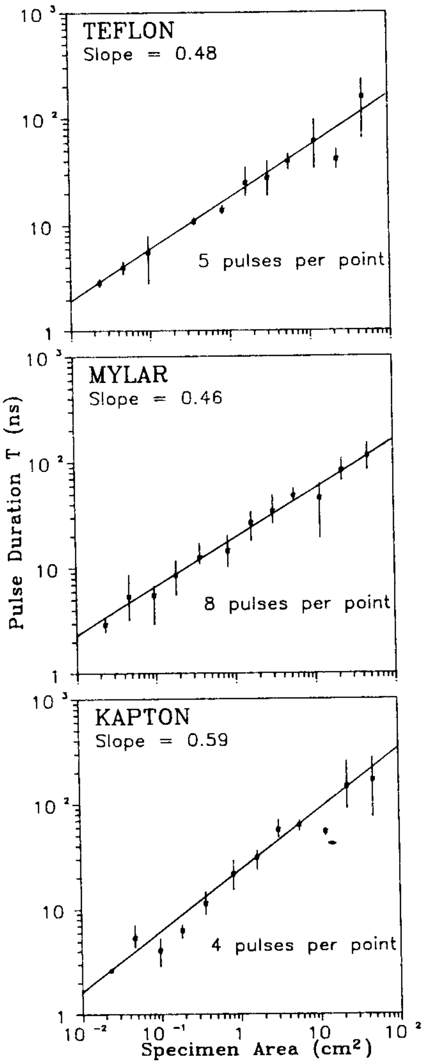

Fig. 7. The arc discharge current pulse duration, showing its approxiately square-root dependence on specimen area [42].

[47] and arc discharging [48], with the conclusion that arc strength was reduced in thin specimens by punchthrough formation and in thick specimens by conductivity effects.

The electron population at synchronous orbit includes a significant fraction with energies high enough to penetrate into a spacecraft's interior, and perhaps cause discharges. Monoenergetic, low-flux beams in the 200–500 keV range were scattered by a 1-mil (25-μm) foil and produced discharges in a circuit board [49]. Combined low-energy non-penetrating and high-energy penetrating beams generally reduced arc occurrence and strength [50], but with different fluxes and energies, such combined beams actually increased arc strength on Kapton and Mylar [51]. Dual low- and medium-energy beams produced very low surface potentials but with enough embedded charge and internal fields to induce breakdown [52,53], which might explain some of the SCATHA observations. Broad-spectrum beams produced a very wide range of discharge strengths [54,55] but led to the conclusion that monoenergetic beams were still useful for worst-case simulations. In a carefully executed simulation of an experiment on the Combined Release and Radiation Effects Satellite (CRRES) [56], it has been shown that discharges occur in many types of dielectrics behind either 3 mils of stainless steel or 8 mils of aluminum.

4. Arc propagation

Arc propagation is the phenomenon that mobilizes large quantities of charge, turning what might otherwise be a small and harmless spark into an arc carrying currents of hundreds or even thousands of amperes. Arc propagation velocities have been measured in different circumstances and by different means, usually resulting in values between 10^5 and 10^6 m/s. Early framing-camera photographs of arc evolution in 2-MeV-charged dielectric blocks revealed some velocity dependence on deposited charge density [57]. A novel "interference" technique for velocity measurement involved arc propagation in opposite directions around a dielectric ring [58]. A segmented-substrate method has been used [59] but this instrumentation method may have influenced the progress of the arcs. Direct measurements of propagation velocity using optical fibers and avalanche photodiode detectors have been made (Fig. 8), after rubbing the specimens very lightly to induce straight arcs and using narrow-aperture masks to generate single arcs [60].

In review papers [61,62], Frederickson presented arguments to the effect that the observed discharge effects can be explained in terms of pre-breakdown streamer formation. Such streamer formation in the bulk of a dielectric has been analyzed [63], resulting in the calculated velocity of 1.65×10^5 m/s in Teflon. A simpler theory [64] associates the high-field failure of the theoretical model with the onset of arc breakdown. However, such bulk models may not be applicable to near-surface arcs on thin materials, arcs which result in the ejection of large quantities of charged particles. Electron ejection (or "blowoff") clearly gives rise to the very high substrate currents that have been measured. There is also evidence for ion emission [65–67], leading to the conclusion that a surface discharge results in the ejection of high-energy electrons and a relatively low-energy plasma of both electrons and ions. The idea that particle motions over the dielectric surface controlled the arc propagation process was expressed in the "brushfire" propagation model [68]. The impor-

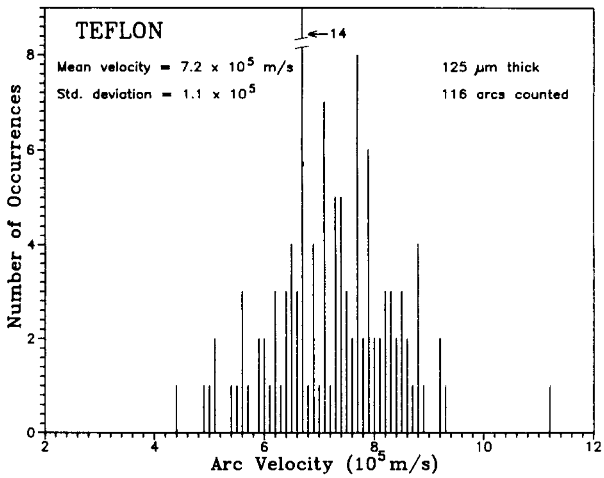

Fig. 8. Arc velocity measurements on Teflon, as measured using optical fibers connected to avalanche photodiodes [60].

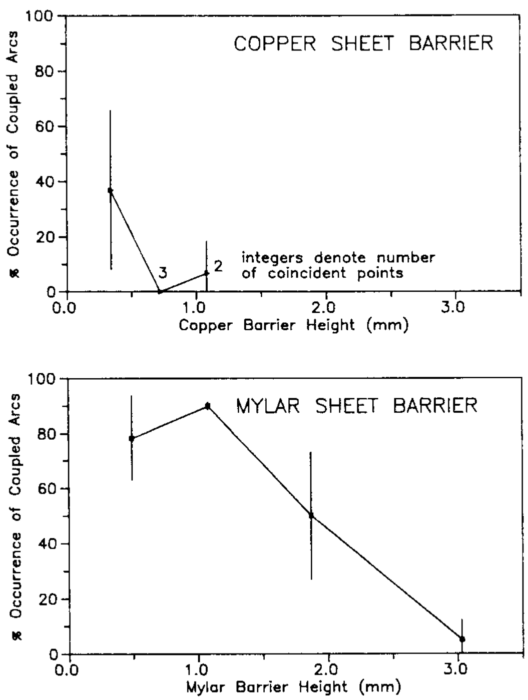

Fig. 9. The effectiveness as an arc barrier of a thin copper sheet and a thin Mylar film. The relative ineffectiveness of the Mylar film barrier suggests that the arc's fields (rather than its ejected particles) trigger the ongoing arc on the other side of the barrier [71].

tance of ion acceleration over the dielectric surface ahead of the breakdown region has been emphasized in recent theoretical work [69,70] which contends that these ions, upon impacting the surface, generate both secondary electrons to discharge the material and secondary ions to advance the discharge wave. However, experimental research on arc barriers [71] (Fig. 9) indicates that the progress of an arc is relatively little impeded by a thin dielectric "wall" which presumably is opaque to particles and transparent to electromagnetic fields; this suggests that the ion acceleration (which indeed must occur in the direction of propagation) is not as important as the local electromagnetic field in advancing the breakdown wave.

5. Electromagnetic interference

The electrons emitted from a propagating arc are strongly accelerated in the field of the undischarged, embedded electrons. The accelerated electrons move tangentially to the surface, to eventually return through whatever return path is available, creating a current loop which forms the source of electromagnetic interference [72–74]; in the case of laboratory models of spacecraft, the measured return currents on the spacecraft body correlate well with numerical computations which begin with the measured properties of the arc discharge. The subject of interference coupling by this mechanism has been reviewed recently in considerable detail [75]. It has also been found through laboratory experiments [76] that direct electromagnetic radiation from arcs on fiberglass struts comes close to specified spacecraft upper limits for radiated interference.

6. Recent developments

The advent of high-voltage solar cell arrays has raised concern about electrical breakdown. It has become established that negative metal (solar cell interconnects) in the vicinity of dielectrics (solar cell cover glass or dielectric supports) gives rise to arc breakdown [77–79]. In particular the existence of an ambient plasma has been established as an important element in this breakdown process [80–82]. It has been suggested that unneutralized surface ions on the metal surface cause high local fields which initiate the discharge [83]. In addition, it has been shown that ambient ions are strongly attracted to electron-charged dielectrics and the ion trajectories are such that the ion beam concentrates into a central spot on the dielectric [48]; charge neutralization apparently occurs in this "ion spot" region because subsequent arcs avoid the region, the overall result being a decrease in the strength of dielectric surface arcs due to the presence of ambient ions [84].

7. Conclusions

The state of the art is that the properties of propagating surface arcs are well known empirically but there is not yet a widely accepted theoretical model for these arcs. A similar statement is valid for propagating subsurface arcs. Surface arc occurrence can be reduced on exposed spacecraft thermal control materials by lightly metallizing the outermost dielectric, although arc occurrence under the metallization is still possible. Surface negative charge accumulation on exposed spacecraft materials will be reduced by the attraction of ambient positive ions, but the available ion flux may not be sufficient for complete neutralization. The accumulation of very-high-energy electrons in cables and circuit boards inside a spacecraft has now been proven to result in arc discharges; such arcs are much smaller than propagating surface or near-surface arcs, but these interior arcs can be just as damaging because the resulting interference signals are channelled to sensitive circuits by the cables and circuit boards on which the arcs occur.

References

1 A. Rosen (Ed.), Spacecraft Charging by Magnetospheric Plasmas, Prog. Astronaut. Aeronaut., AIAA, Vol. 47, 1976.
2 H.B. Garrett and C.P. Pike (Eds.), Space Systems and Their Interactions with Earth's Space Environment, Prog. Astronaut. Aeronaut., AIAA, Vol. 71, 1980.
3 C.P. Pike and R.R. Lovell (Eds.), Proceedings of the Spacecraft Charging Technology Conference, Report AFGL-TR-77-0051/NASA TMX-73537, Conference held in Colorado Springs, CO, 27-29 Oct. 1976.
4 J.M. Goodman (Ed.), Effect of the Ionosphere on Space and Terrestrial Systems, Proceedings of an NRL/ONR Symposium held in Arlington, VA, 24-26 Jan. 1978, US GPO No. 0-277-182.
5 R.C. Finke and C.P. Pike (Eds.), Spacecraft Charging Technology - 1978, Report AFGL-TR-79-0082/NASA Conference Publication 2071, Proceedings of a Conference held in Colorado Springs, CO, 31 Oct.-2 Nov. 1978.
6 N.J. Stevens and C.P. Pike (Eds.), Spacecraft Charging Technology - 1980, Report AFGL-TR-81-0270/NASA Conference Publication 2182, Proceedings of a Conference held in Colorado Springs, CO, 12-14 Nov. 1980.
7 C.K. Purvis and C.P. Pike (Eds.), Spacecraft Environmental Interactions Technology - 1983, Report AFGL-TR-85-0018/NASA Conference Publication 2359, Proceedings of a Conference held in Colorado Springs, CO, 4-6 Oct. 1983.
8 A. Rosen, Spacecraft charging by magnetospheric plasma, IEEE Trans. Nucl. Sci., NS-23 (1976) 1762-1768.
9 D.A. McPherson and W.R. Schober, Spacecraft charging at high altitudes: the SCATHA satellite program, in Ref. [1], pp. 15-30.
10 R.R. Shaw, J.E. Nanevicz and R.C. Adamo, Observations of electrical discharges caused by differential satellite-charging, in Ref. [1], pp. 61-76.
11 H.B. Garrett, Spacecraft charging: a review, in Ref. [2], pp. 167-226.
12 S.E. DeForest, The plasma environment at geosynchronous orbit, in Ref. [3], pp. 37-52.
13 J.B. Reagan, R.E. Meyerott, E.E. Gaines, R.W. Nightingale, P.C. Filbert and W.L. Imhof, Space charging currents and their effects on spacecraft systems, IEEE Trans. Electr. Insul., EI-18 (1983) 354-365.

14 M.S. Gussenhoven and E.G. Mullen, Geosynchronous environment for severe spacecraft charging, J. Spacecr. Rockets, 20 (1983) 26-34.
15 J.L. Horowitz, Dynamics of magnetospheric plasmas, J. Spacecr. Rockets, 22 (1985) 225-230.
16 H.B. Garrett and G.C. Spitale, Magnetospheric plasma modeling (0-100 keV), J. Spacecr. Rockets, 22 (1985) 231-244.
17 P.L. Leung, G.H. Plamp and P.A. Robinson, Galileo internal electrostatic discharge program, in Ref. [7], pp. 423-435.
18 S.E. DeForest, Spacecraft charging at synchronous orbit, J. Geophys. Res., 77 (1972) 651-659.
19 W.L. Lehn, SCATHA conductive spacecraft materials development, J. Spacecr. Rockets, 20 (1983) 182-186.
20 W.R. Elkman, E.M. Brown, D.V.Z. Wadsworth, E.C. Smith and P.F. Adams, Electrostatic charging and radiation shielding design philosophy for a synchronous satellite, J. Spacecr. Rockets, 20 (1983) 417-424.
21 H.C. Koons, Summary of environmentally induced electrical discharges on the P78-2 (SCATHA) satellite, J. Spacecr. Rockets, 20 (1983) 425-431.
22 R.C. Adamo and J.R. Mattarese, Transient pulse monitor data from the P78-2 (SCATHA) spacecraft, J. Spacecr. Rockets, 20 (1983) 432-437.
23 P.F. Mizera, A summary of spacecraft charging results, J. Spacecr. Rockets, 20 (1983) 438-443.
24 B. Gross, Irradiation effects in borosilicate glass, Phys. Rev., 107 (1957) 368-373.
25 B. Gross, Irradiation effects in Plexiglas, J. Polym. Sci., 27 (1958) 135-143.
26 N.J. Stevens, R.R. Lovell and V. Gore, Spacecraft-charging investigation for the CTS project, in Ref. [1], pp. 263-275.
27 M. Gossland, K.G. Balmain and M.J. Treadaway, Surface flashover arc orientation on Mylar film, IEEE Trans. Nucl. Sci., NS-28 (1981) 4535-4540.
28 E.J. Yadlowsky, R.C. Hazelton and R.J. Churchill, Characteristics of edge break-downs on Teflon samples, IEEE Trans. Nucl. Sci., NS-27 (1980) 1765-1769.
29 J. Dauphin and T.D. Guyenne (Eds.), Spacecraft Materials in Space Environment, Report ESA SP-145, Proceedings of a Symposium held at Noordwijk, The Netherlands, 2-5 Oct. 1979.
29a K.G. Balmain, Surface discharge arc propagation and damage on spacecraft dielectrics, in Ref. [29], pp. 209-215.
30 A. Rolfo, J. Dauphin and T.D. Guyenne (Eds.), Spacecraft Materials in a Space Environment, Report ESA SP-178, Proceedings of a Symposium held in Toulouse, France, 8-11 June 1982.
30a O. Berolo, Damage and deterioration of Teflon second-surface mirrors by space simulated electron irradiation, in Ref. [30], pp. 231-240.
30b K.G. Balmain, M. Gossland, R.D. Reeves and W.G. Kuller, Phenomenology of surface arcs on spacecraft dielectric materials, in Ref. [30], pp. 263-268.
31 B.R.F. Kendall, Mass spectra of neutral particles released during electrical break-down of thin polymer films, in Ref. [7], pp. 525-535.
32 J.E. Nanevicz and R.C. Adamo, Occurrence of arcing and its effect on space systems, in Ref. [2], pp. 252-275.
33 R.D. Reeves and K.G. Balmain, Two-dimensional electron beam charging model for polymer films, IEEE Trans. Nucl. Sci., NS-28 (1981) 4547-4552.
34 C.N. Fellas and S. Richardson, Internal charging of indium oxide coated mirrors, IEEE Trans. Nucl. Sci., NS-28 (1981) 4523-4528.
35 V.A.J. van Lint, D.A. Fromme and R. Stettner, Skynet satellite electron precharging experiments, in Ref. [5], pp. 587-605.
36 V.A.J. van Lint, B.C. Passenheim, R. Stettner and D.A. Fromme, The effect of electron precharging on SGEMP response of insulators, IEEE Trans. Nucl. Sci., NS-26 (1979) 5024-5029.
37 E.J. Yadlowsky and R.C. Hazelton, Studies of microdamage in dielectric discharges, J. Spacecr. Rockets, 22 (1985) 282-286.

38 E.R. Williams, C.M. Cooke and K.A. Wright, Electrical discharge propagation in and around space charge clouds, J. Geophys. Res., 90 (1985) 6059-6070.

39 K.G. Balmain, P.C. Kremer and M. Cuchanski, Charged-area effects on spacecraft dielectric arc discharges, in Ref. [4], pp. 302-308.

40 K.G. Balmain, Scaling laws and edge effects for polymer surface discharges, in Ref. [5], pp. 646-656.

41 K.G. Balmain, Surface discharge effects in Ref. [2], pp. 276-298.

42 K.G. Balmain and G.R. Dubois, Surface discharges on Teflon, Mylar and Kapton, IEEE Trans. Nucl. Sci., NS-26 (1979) 5146-5151.

43 P. Leung and G. Plamp, Characteristics of RF resulting from dielectric discharges, IEEE Trans. Nucl. Sci., NS-29 (1982) 1610-1614.

44 P.L. Leung, Characteristics of electromagnetic interference generated during discharge of Mylar samples, IEEE Trans. Nucl. Sci., NS-31 (1984) 1587-1590.

45 T.M. Flanagan, R. Denson, C.E. Mallon, M.J. Treadaway and E.P. Wenaas, Effect of laboratory simulation parameters on spacecraft dielectric discharges, IEEE Trans. Nucl. Sci., NS-26 (1979) 5134-5140.

46 K.G. Balmain and W. Hirt, Dielectric surface discharges: dependence on incident electron flux, IEEE Trans. Nucl. Sci., NS-27 (1980) 1770-1775.

47 W.S. Williamson, C.R. Dulgeroff, J. Hymann and R. Viswanathan, Kapton charging characteristics: effects of material thickness and electron-energy distribution, in Ref. [7], pp. 547-558.

48 K.G. Balmain, A. Battagin and G.R. Dubois, Thickness scaling for arc discharges on electron-beam-charged dielectrics, IEEE Trans. Nucl. Sci., NS-32 (1985) 4073-4078.

49 E.P. Wenaas, M.J. Treadaway, T.M. Flanagan, C.E. Mallon and R. Denson, High-energy electron-induced discharges in printed circuit boards, IEEE Trans. Nucl. Sci., NS-26 (1979) 5152-5155.

50 M.J. Treadaway, C.E. Mallon, T.M. Flanagan, R. Denson and E.P. Wenaas, The effects of high-energy electrons on the charging of spacecraft dielectrics, IEEE Trans. Nucl. Sci., NS-26 (1979) 5103-5106.

51 K.G. Balmain and W. Hirt, Dielectric surface discharges: effects of combined low-energy and high-energy incident electrons, IEEE Trans. Electr. Insul., ES-18 (1983) 498-503.

52 M.S. Leung, M.B. Tueling and E.R. Schnauss, Effects of secondary emission on charging, in Ref. [6], pp. 163-178.

53 P. Coakley, B. Kitterer and M. Treadaway, Charging and discharging characteristics of dielectric materials exposed to low- and mid-energy electrons, IEEE Trans. Nucl. Sci., NS-29 (1982) 1639-1643.

54 P. Coakley, M. Treadaway, N. Wild and B. Kitterer, Discharge characteristics of dielectric materials examined in mono-, dual-, and spectral energy electron charging environments, in Ref. [7], pp. 511-524.

55 P.G. Coakley, N. Wild and M.J. Treadaway, Laboratory investigation of dielectric materials exposed to spectral electron environments (1 to 100 keV), IEEE Trans. Nucl. Sci., NS-30 (1983) 4605-4609.

56 P.G. Coakley, M.J. Treadaway and P.A. Robinson, Jr., Low flux laboratory test of the internal discharge monitor (IDM) experiment intended for CRRES, IEEE Trans. Nucl. Sci., NS-32 (1985) 4066-4072.

57 L.M. Erickson and D.C. Oakley, Time-resolved voltage breakdown in various insulators due to 2-MeV electrons, Report UCRL-51372, Lawrence Livermore Laboratory, Univ. of California at Livermore, 5 April 1973.

58 C.M. Cooke, E. Williams and K.A. Wright, Electrical discharge propagation in space-charged PMMA, Conference Record of the 1982 IEEE Int. Symposium on Electrical Insulation, pp. 95-101.

59 B.C. Passenheim, V.A.J. van Lint, J.D. Riddell and R. Kitterer, Electrical conductivity and discharge in spacecraft thermal control dielectrics, IEEE Trans. Nucl. Sci., NS-29 (1982) 1594-1600.

60 K.G. Balmain, M. Gossland, R.D. Reeves and W.G. Kuller, Optical measurement of the velocity of dielectric surface arcs, IEEE Trans. Nucl. Sci., NS-29 (1982) 1615-1617.
61 A.R. Frederickson, Electric discharge pulses in irradiated solid dielectrics in space, IEEE Trans. Electr. Insul., EI-18 (1983) 337-349.
62 A.R. Frederickson, Discharge pulse phenomenology, in Ref. [7], pp. 483-509.
63 B.L. Beers, V.W. Pine, H.C. Hwang and H.W. Bloomberg, Negative streamer development in FEP Teflon, IEEE Trans. Nucl. Sci., NS-26 (1979) 5127-5133.
64 B.L. Beers, R.E. Daniell and T.N. Delmer, A simple model of electron beam initiated dielectric breakdown, in Ref. [7], pp. 591-598.
65 E.J. Yadlowsky, R.C. Hazelton and R.J. Churchill, Characteristization of electrical discharges on Teflon dielectrics used as spacecraft thermal control surfaces, in Ref. [5], pp. 632-645.
66 R.C. Hazelton, R.J. Churchill and E.J. Yadlowsky, Measurements of particle emission from discharge sites in Teflon irradiated by high energy electron beams, IEEE Trans. Nucl. Sci., NS-26 (1979) 5141-5145.
67 N. Wild and P. Coakley, Evidence for discrete plasma emission during dielectric discharge events, IEEE Trans. Nucl. Sci., NS-31 (1984) 1591-1593.
68 G.T. Inouye, Brushfire arc discharge model, in Ref. [6], pp. 133-162.
69 R. Stettner and G. Duerksen, The discharge of spacecraft dielectrics and the theory of Lichtenberg figure formation, IEEE Trans. Nucl. Sci., NS-31 (1984) 1375-1380.
70 R. Stettner and A.B. DeWald, A surface discharge model for spacecraft dielectrics, IEEE Trans. Nucl. Sci., NS-32 (1985) 4079-4086.
71 M. Gossland and K.G. Balmain, Barriers to flashover discharge arcs on Teflon, IEEE Trans. Nucl. Sci., NS-29 (1982) 1618-1620.
72 M.J. Treadaway, A.J. Woods, T.M. Flanagan, R.E. Leadon, R. Grismore, R. Denson and E.P. Wenaas, Experimental verification of an ECEMP spacecraft discharge coupling model, IEEE Trans. Nucl. Sci., NS-27 (1980) 1776-1779.
73 I. Katz, M.J. Mandell, D.E. Parks and G.W. Schnuelle, A theory of dielectric surface discharges, IEEE Trans. Nucl. Sci., NS-27 (1980) 1786-1791.
74 R. Stettner, R. Marks and J. Dancz, Physical modeling of spacecraft discharge processes and associated electron blowoff, IEEE Trans. Nucl. Sci., NS-27 (1980) 1780-1785.
75 A.J. Woods and E.P. Wenaas, Spacecraft discharge electromagnetic interference coupling models, J. Spacecr. Rockets, 22 (1985) 265-281.
76 K.G. Balmain, M. Gossland and K. Karia, Spacecraft fiberglass strut charging/discharging and EMI, IEEE Trans. Nucl. Sci., NS-32 (1985) 4438-4440.
77 R.C. Chaky and G.T. Inouye, Characteristics of EMI generated by negative metal/positive dielectric voltage stresses due to spacecraft charging, in Ref. [7], pp. 437-451.
78 W.L. Miller, An investigation of arc discharging on negatively biased dielectric-conductor samples in a plasma, in Ref. [7], pp. 367-377.
79 G.T. Inouye and R.C. Chaky, Enhanced electron emission from positive dielectric/negative metal configurations on spacecraft, IEEE Trans. Nucl. Sci., NS-29 (1982) 1589-1593.
80 D.B. Snyder, Discharges on a negatively biased solar cell array in a charged-particle environment, in Ref. [7], pp, 379-388.
81 D.B. Snyder, Environmentally induced discharges in a solar array, IEEE Trans. Nucl. Sci., NS-29 (1982) 1607-1609.
82 D.B. Snyder, Characteristics of arc currents on a negatively biased solar cell array in a plasma, IEEE Trans. Nucl. Sci., NS-31 (1984) 1584-1587.
83 G.A. Jongeward, I. Katz, M.J. Mandell and D.E. Parks, The role of unneutralized surface ions in negative potential arcing, IEEE Trans. Nucl. Sci., NS-32 (1985) 4087-4091.
84 M. Gossland and K.G. Balmain, Incident ion effects on polymer surface discharges, IEEE Trans. Nucl. Sci., NS-30 (1983) 4302-4306.